Supplemental Tables, Figures, and Movies:

Table S1: Pair-wise comparison of FG domain properties using the Tukey HSD test. Statistical analyses of nup properties calculated from the MD trajectories. These included the average Rg value (over each 3 ns simulation), the standard deviation of the Rg (over each 3 ns simulation), the average shape parameter (S), the standard deviation of the S value, the order parameter (S^2) (averaged over all residues), and the *frequency spectrum* of the Rg and S time series for each of the MD simulations.

Figure S1: Purified FG domains of nups. Large (**A**) and small (**B**) FG domains of nups were isolated as described in the Experimental Procedures. The isolated FG domains were resolved by SDS-PAGE, and stained with Coomassie blue. Red arrows point to FG domains. Other bands are GST or FG domain fragments. Not all of the purified FG domains analyzed are shown in these sample gels.

Figure S2: Structural fluctuations in the simulated FG domains. Plots showing the root-mean-square deviation (in Angstroms) of backbone C-alpha carbons relative to the first structure in the final 3 ns of each replicate trajectory at 300K. Separate lines are shown for each of the 40 replicate simulations. The plots show that most replicates for each protein continue to exhibit large-scale motions throughout the simulation, as expected for disordered proteins.

Figure S3: Secondary structures in the simulated FG domains. (***A***) Content of secondary structures adopted by the FG domains during the final 3 ns of the simulations at 300K. The data was obtained by analyzing structures sampled every 300 ps across all 40 simulations for each FG domain (400 structures in total) using the program DSSP, which assigns each residue to a particular secondary structure class [1]. The results are displayed as the aggregate of all 40 replicates for each FG domain. Note that secondary structure elements typically found in folded proteins *(i.e.* beta sheet and alpha helix) are underrepresented in the FG domains. Similar results were obtained from simulations at 350K (not shown). **(*B*)** Per-residue contribution to helical secondary structure detected in the FG domains. Each color indicates the contribution of one of the forty replicates to the helical content at that location. The graphs show that the 3-10 and alpha helix structures detected are present in some simulations for a fraction of the time (the remaining time is spent in highly flexible configurations), but not in all of the simulations all of the time. Interestingly however, the location of the helical structures along the polypeptide chain is consistent in all replicates. The 'valleys' in the histogram mark highly-flexible segments

with no structure or sharp bends. Similar results were obtained from simulations at 350K (not shown).

Figure S4: The *stalk* regions of Nup116, Nup100 and Nup145 are intrinsically-disordered. (**A**) The *stalk* regions of Nup116, Nup100 and Nup145 are hypersensitive to proteases. Purified nup domains (2 mg/ml) and Kap60 (2 mg/ml) (a folded protein with a ~50 AA unstructured N-terminus) were dissolved in 20 mM Hepes pH 6.8, 150 mM KOAc, 2 mM $Mg(OAc)_2$, and were digested with 100 ng/ml of proteinase K at 37ºC. Aliquots were removed from the incubation at time intervals, and the reactions were quenched with 2% SDS plus 2 mM PMSF followed by heating at 95ºC for 10 min. The digested proteins were resolved by SDS-PAGE and stained with Coomassie blue. Note that the disordered domains are completely degraded during the time course, while the folded Kap60 is not, except for its unstructured N-terminus explaining the slight reduction in its MW. (**B**) CD measurements of nup *stalk* regions produce spectra characteristic of intrinsically-disordered proteins. Far-UV CD spectra of purified nup domains in phosphate buffer at neutral pH were obtained at 25°C on a BioLogic MOS-450 CD instrument. Spectra were recorded using 0.01 cm cuvette from 250 to 190 nm with a step size of 1 nm and an averaging time of 10 s. For all spectra, an average of three scans was obtained and the background spectra of the buffer were removed. Note that each nup domain has an intensive minimum near 200 nm and low ellipticity at 222 nm, which reflect extensive contribution of unstructured coil and a lack of alpha-helical structure.

Movie S1 and S2: Structural dynamics of intrinsically-disordered FG domains. Movies of the small Nup116 FG domain (AA 348-458) (**Movie S1**) and the small Nsp1 FG domain (AA 375-479) (**Movie S2**) were generated from MD simulations using the Visual Molecular Dynamics (VMD) software package. Structures were sampled every 1 ps for the final 1 ns of 350K dynamics and the resulting frames were combined at 15 frames/sec for a total movie duration of ~1 min. Principal Components Analysis was applied to each structure and was then used to rotate the first two principal components onto the viewing plane for more effective visualization of the dynamics.

References:

1. Kabsch, W. and C. Sander, *Dictionary of Protein Secondary Structure: Pattern Recognition of Hydrogen-Bonded and Geometrical Features.* Biopolymers 1983. **22**.

Table S1. Pair-wise comparison of FG domain properties using the Tukey HSD test.

Pair-wise comparison	**Rg**			**S**			
between the small FG domains	**mean**	**s.d.**	**freq. band**	**mean**	**s.d.**	**freq. band**	S^2
Nsp1 FxFG vs Nup116 GLFG	0.0537	0.0275	0.0046	0.9842	0.9168	0.9853	0.0057
Nsp1 FxFG vs Nup116 GLFG charged	0.4753	0.9995	0.0282	1	1	0.9997	0.7852
Nsp1 FxFG vs Nsp1 SxSG	0	0	0	0	0	0	0
Nup116 GLFG vs Nup116 GLFG charged	0.0005	0.0375	0	0.9785	0.915	0.9938	0.0002
Nsp1 SxSG vs Nup116 GLFG	0	0	0	0	0	0	0
Nsp1 SxSG vs Nup116 GLFG charged	0	0	0	0	0	0	0
Mean p-value	0.0883	0.1774	0.0055	0.4938	0.472	0.4965	0.1318

Low p-values (< 0.05) indicated statistically-significant differences for a particular property between two different FG domains.

Figure S1

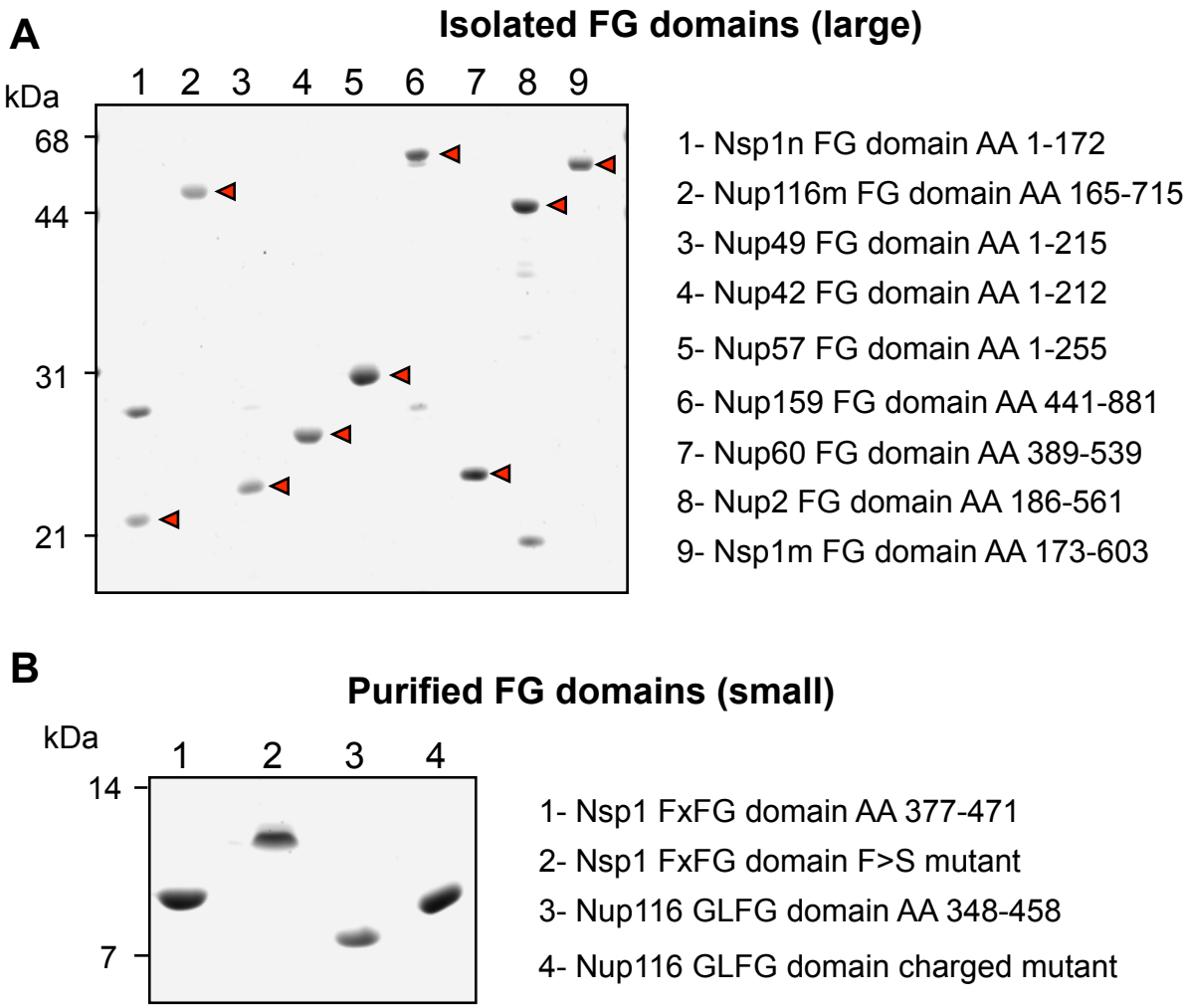
A
Isolated FG domains (large)
kDa
1 2 3 4 5 6 7 8 9
68
44
31
21
1- Nsp1n FG domain AA 1-172
2- Nup116m FG domain AA 165-715
3- Nup49 FG domain AA 1-215
4- Nup42 FG domain AA 1-212
5- Nup57 FG domain AA 1-255
6- Nup159 FG domain AA 441-881
7- Nup60 FG domain AA 389-539
8- Nup2 FG domain AA 186-561
9- Nsp1m FG domain AA 173-603
B
Purified FG domains (small)
kDa
1 2 3 4
14
7
1- Nsp1 FxFG domain AA 377-471
2- Nsp1 FxFG domain F>S mutant
3- Nup116 GLFG domain AA 348-458
4- Nup116 GLFG domain charged mutant

Figure S2

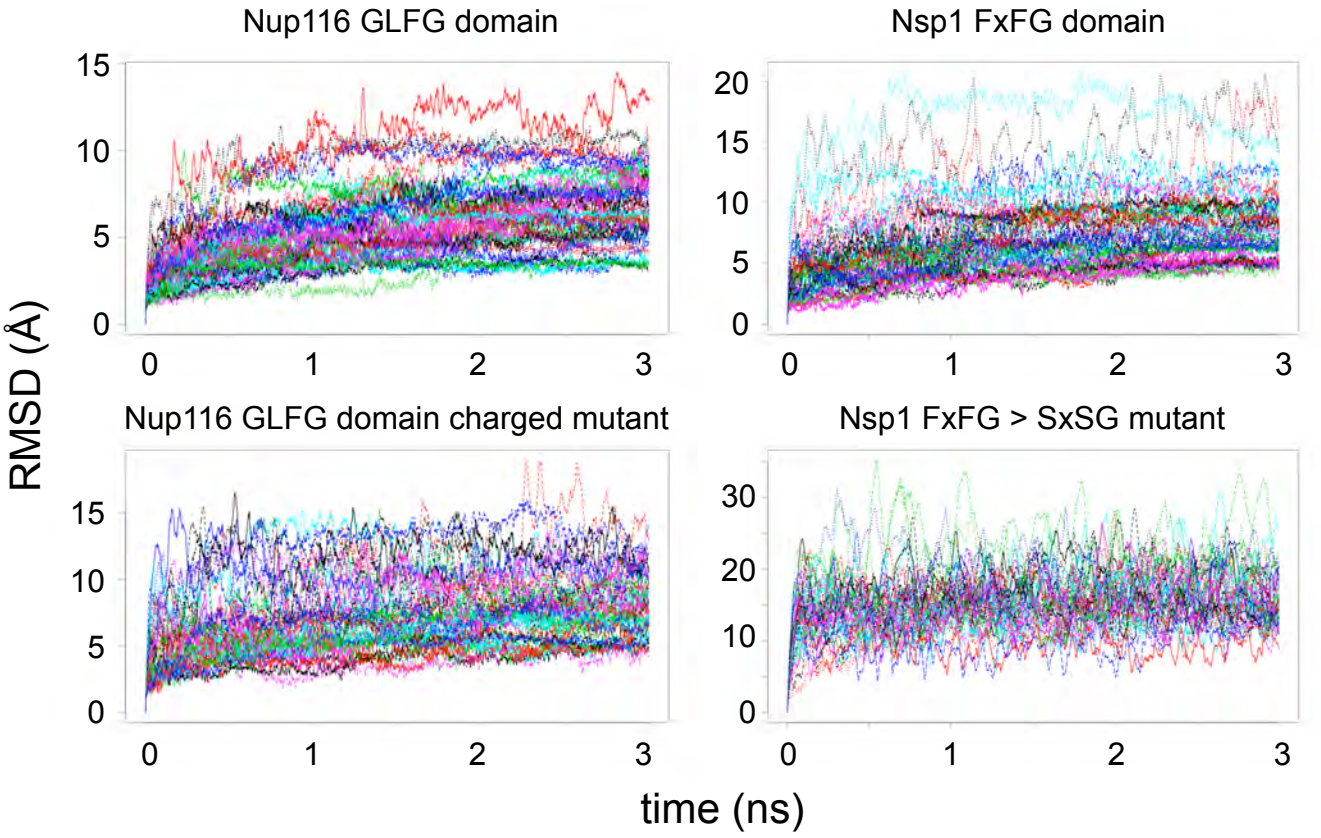
Nup116 GLFG domain
Nsp1 FxFG domain
Nup116 GLFG domain charged mutant
Nsp1 FxFG > SxSG mutant
RMSD (Å)
time (ns)
0
5
10
15
20
30
1
2
3

Figure S3

A

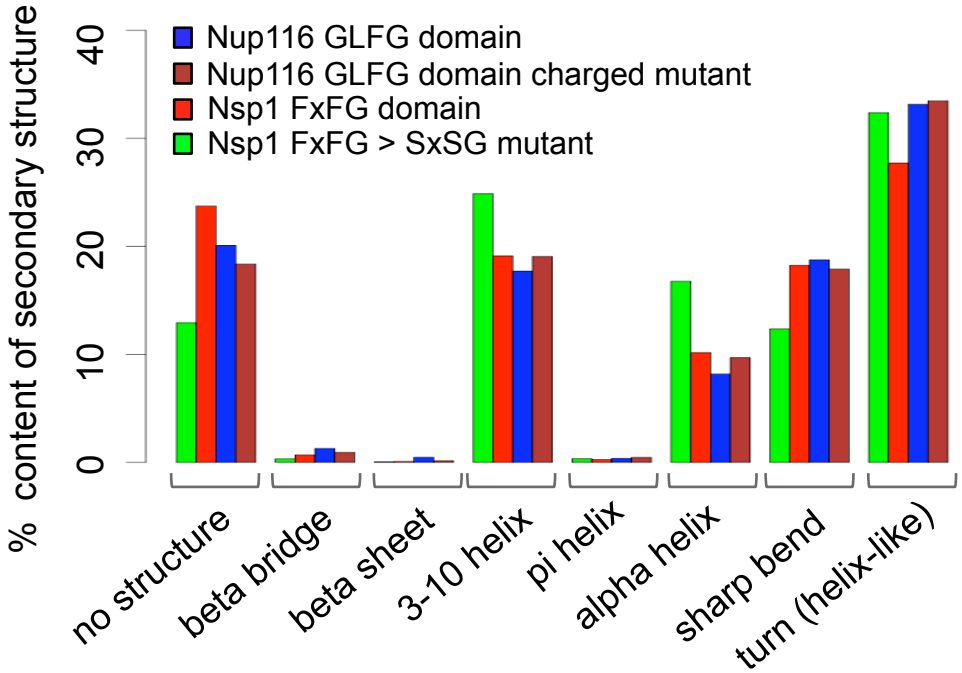
% content of secondary structure
0
10
20
30
40
Nup116 GLFG domain
Nup116 GLFG domain charged mutant
Nsp1 FxFG domain
Nsp1 FxFG > SxSG mutant
no structure
beta bridge
beta sheet
3-10 helix
pi helix
alpha helix
sharp bend
turn (helix-like)

B

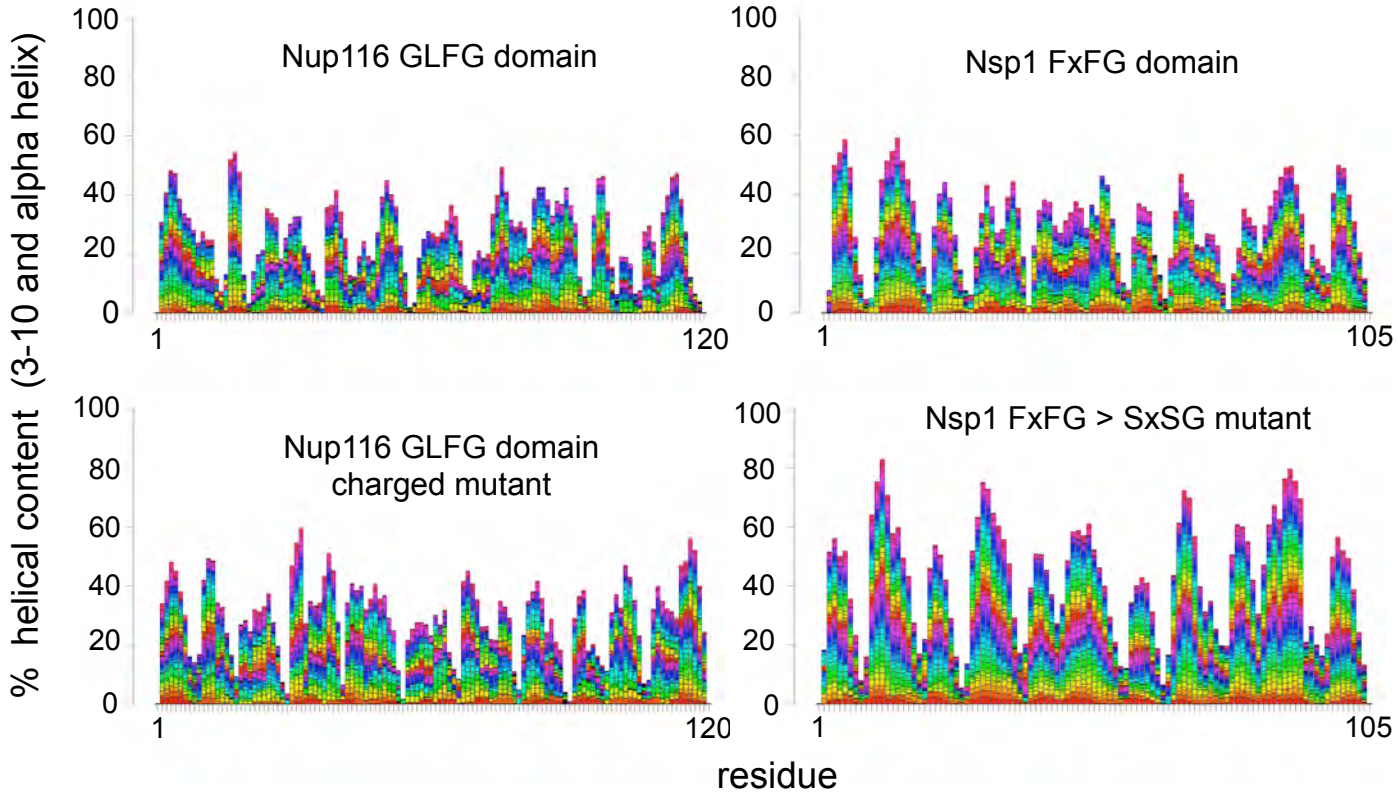
% helical content (3-10 and alpha helix)
Nup116 GLFG domain
Nsp1 FxFG domain
Nup116 GLFG domain
charged mutant
Nsp1 FxFG > SxSG mutant
0
20
40
60
80
100
1
120
105
residue

Figure S4

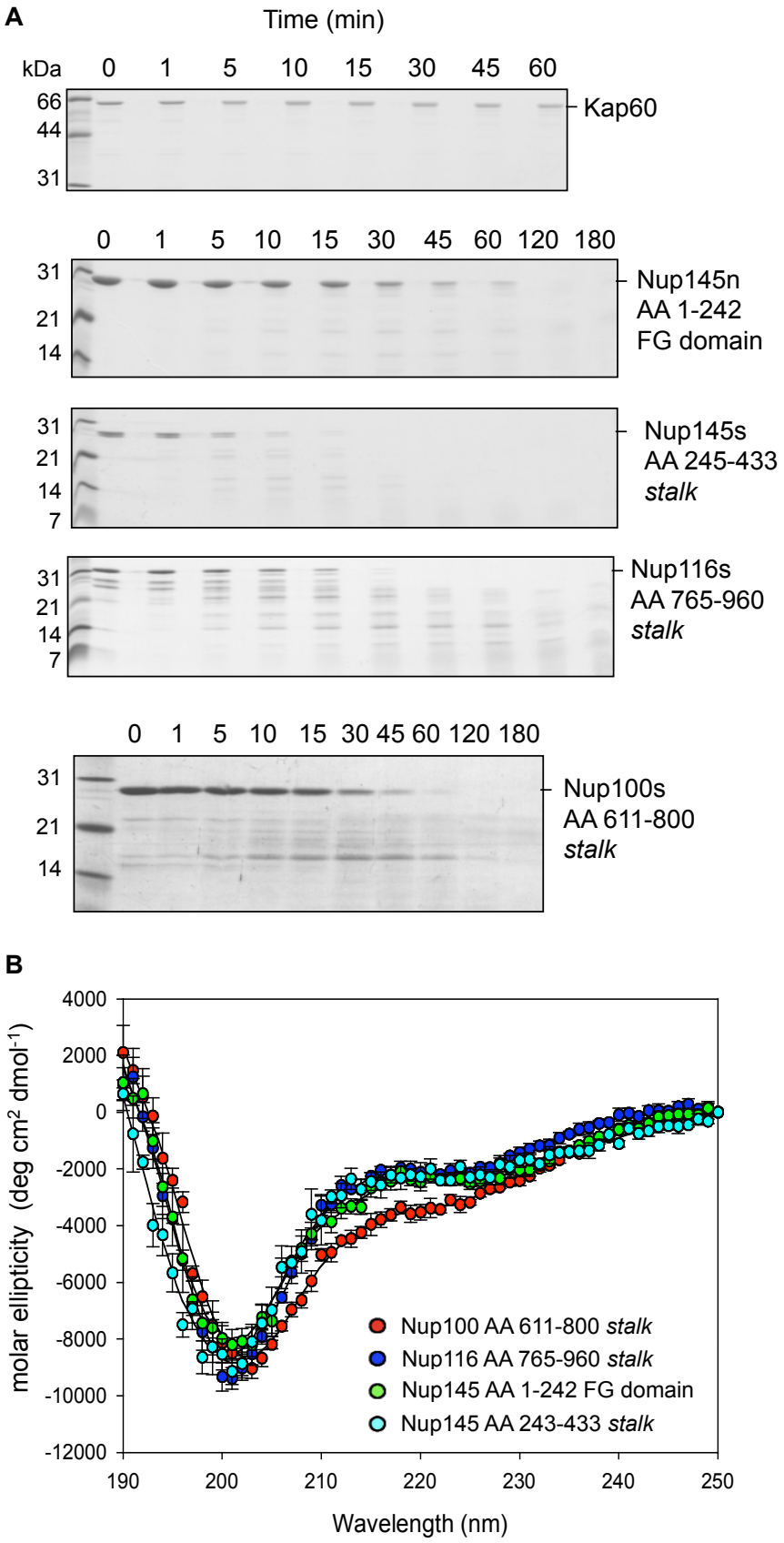
A
Time (min)
kDa
0 1 5 10 15 30 45 60
66
44
31
Kap60
0 1 5 10 15 30 45 60 120 180
31
21
14
Nup145n
AA 1-242
FG domain
31
21
14
7
Nup145s
AA 245-433
stalk
31
21
14
7
Nup116s
AA 765-960
stalk
0 1 5 10 15 30 45 60 120 180
31
21
14
Nup100s
AA 611-800
stalk
B
molar ellipticity (deg cm2 dmol-1)
4000
2000
0
-2000
-4000
-6000
-8000
-10000
-12000
190
200
210
220
230
240
250
Wavelength (nm)
Nup100 AA 611-800 stalk
Nup116 AA 765-960 stalk
Nup145 AA 1-242 FG domain
Nup145 AA 243-433 stalk